Volume: 11 Issues: 87 Special Issue [October, 2026] pp 951-965
Journal of Islamic, Social, Economics and Development (JISED)
eISSN: 0128-1755
Journal website: academicinspired.com/jised
DOI: 10.55573/JISED.118765

A PARAMETRIC EVALUATION AND GRID-RESOLUTION STUDY OF THE KORTEWEG–DE VRIES EQUATION USING THE FOURIER PSEUDOSPECTRAL METHOD

Nik Nur Amiza Nik Ismail[1*]
Azwani Alias[2]

[1] Faculty of Computer and Mathematical Sciences, Universiti Teknologi MARA Kelantan, 18500, Machang, Kelantan, Malaysia (niknuramiza@uitm.edu.my)
[2] Special Interest Group on Modelling and Data Analytics (SIGMDA), Faculty of Computer Science and Mathematics, Universiti Malaysia Terengganu, 21030 Kuala Nerus, Terengganu, Malaysia (azwani.alias@umt.edu.my)
*Corresponding author: niknuramiza@uitm.edu.my

Article history
Received date : 10-9-2026
Revised date : 10-9-2026
Accepted date : 17-10-2026
Published date : 25-10-2026

To cite this document:
Nik Ismail, N. N. A., & Alias, A. (2026). A parametric evaluation and grid-resolution study of the Korteweg–de Vries equation using the Fourier pseudospectral method. *Journal of Islamic, Social, Economics and Development (JISED),* 11 (87), 951-965.

Abstract: *The Fourier pseudospectral method is a well-established numerical approach for solving partial differential equations (PDEs). One of the most well-known PDEs is the classical Korteweg–de Vries (KdV) equation which models shallow-water wave systems such as tsunamis and tidal bores. The qualitative behaviour of KdV solutions changes accordingly with the relative strengths of nonlinearity and dispersion, and reliable numerical capture of these different regimes depends on spatial resolution, aliasing control, and computational-domain selection. However, these numerical issues are often considered separately rather than systematically within a single Fourier pseudospectral framework. Here, the Fourier pseudospectral method is employed to study the nonlinear dispersive wave propagation. Spatial derivatives are evaluated in Fourier space, while the nonlinear terms are computed in physical space using the standard 2/3 dealiasing rule to reduce aliasing errors. Since the accuracy of this method depends strongly on the spatial resolution, a grid-resolution study is first conducted using different numbers of spatial grid points, N, to determine their influence on the numerical solution. Three parameter regimes are considered to examine the effects of the relative strengths of nonlinearity and dispersion. In the balanced regime, the amplitude and the phase speed of the solitary wave is maintained providing a validation of the numerical implementation and parameter selection. In the nonlinearity-dominated regime, increasing the nonlinear coefficient produces wave steepening followed by soliton fission. Conversely, increasing the dispersion coefficient leads to amplitude reduction, dispersive spreading, and the development of oscillatory wave trains. The results demonstrate that the Fourier pseudospectral method with appropriate spatial resolution and 2/3 dealiasing can accurately resolve qualitatively different KdV wave regimes when computational-domain size is appropriately selected.*

Keywords: *Korteweg–de Vries equation; Fourier pseudospectral method; grid resolution; dealiasing; soliton fission; dispersive waves*

Copyright © Academic Inspired Network - All rights reserved

This work is licensed under CC BY 4.0

Volume: 11 Issues: 87 Special Issue [October, 2026] pp 951-965
Journal of Islamic, Social, Economics and Development (JISED)
eISSN: 0128-1755
Journal website: academicinspired.com/jised
DOI: 10.55573/JISED.118765

Introduction

The Korteweg–de Vries (KdV) equation is a classical nonlinear dispersive partial differential equation (PDE) which describe the propagation of long waves in shallow water is first introduced by Diederik Korteweg and Gustav de Vries (Korteweg & de-Vries, 1895). Its significance lies in its ability to represent the competition between nonlinear wave steepening and dispersion, which can lead to the formation of localized solitary waves. Historically, these waves have been observed by John Scott Russell in 1834, who observed a single wave moving along a canal while approximately maintaining its shape (Singh & Senthilnathan, 2024). Ever since, the KdV equation has emerged as one of the key models for the study of nonlinear dispersive wave propagation and has been the subject of extensive research in mathematical physics and applied mathematics. The general form of the KdV equation is:

$$A_t + \mu A A_x + \lambda A_{xxx} = 0 \quad (1)$$

The amplitude of the wave is denoted by $A(x,t)$ while x is the spatial coordinate, and t is time. Here, the nonlinear term, μ promotes wave steepening, whereas the third-order derivative term, λ causes dispersion. These two terms will have different relative strengths, which will affect the overall wave behaviour. Under proper balanced, the equation admits localized solitary-wave solutions. This theory has been validated in recent studies of KdV-type models and their solitary wave structures (Klein et al.,2023; Ablowitz et al.,2023; Alomair et al, 2025; Biswas et al., 2025). The KdV equation (1) is integrable and yielded to solitary wave solutions given by:

$$A(x,t) = a \sec h^2\left(k\left(x - ct\right)\right), \qquad c = \frac{\mu a}{3} = 4\lambda k^2 \quad (2)$$

where phase speed, c is proportional to the square of the wavenumber, k^2 or the wave amplitude, a indicating that the solitary waves run with an increasing speed of the amplitude of the waves. This solution illustrates the characteristic relationship between amplitude and propagation where the smaller amplitude waves propagating more slowly, and larger amplitude waves are more localized and travelling faster (Irawan et al., 2026).

However, in real phenomenon, the coefficient may vary according to physical structure of topography (Cheng & Liu, 2023). This led to more complex wave behaviour due to the difference in the relative strength of the nonlinear and dispersive effects. If the nonlinear contribution is dominant, the wave steepening is more pronounced and one or more localized structures can be formed by soliton fission. On the other hand, if dispersion is dominant, the wave amplitude decreases and oscillatory structures is formed while increased spatial spreading (Congy et al., 2023; Shamshu, et al., 2025). These different regimes provide a useful framework for examining the numerical capability of a computational method to resolve various nonlinear dispersive wave behaviours. In recent years, numerical studies of KdV and related equations has been continuing to investigate solitary-wave propagation, nonlinear interactions, and dispersive structures including finite-difference, finite-element, discontinuous Galerkin, and spectral methods (Sang & Wu, 2024; Dwivedi & Sarkar, 2025; Wang et al., 2025; Salian et al., 2026).

The numerical accuracy for nonlinear dispersive equations is especially significant due to the possibility of evolution of localized structures, steep gradients, and high-frequency oscillations. According to Irawan et al., (2026), Fourier pseudospectral methods are attractive as spatial derivatives can be evaluated accurately in Fourier space, while the fast Fourier transform (FFT)

Copyright © Academic Inspired Network
- All rights reserved

This work is licensed under
CC BY 4.0

Volume: 11 Issues: 87 Special Issue [October, 2026] pp 951-965
Journal of Islamic, Social, Economics and Development (JISED)
eISSN: 0128-1755
Journal website: academicinspired.com/jised
DOI: 10.55573/JISED.118765

provides an efficient transformation between physical and spectral representations. Recently, numerical studies of KdV-type equations have demonstrated the ability of Fourier pseudospectral approaches in capturing the solitary waves and investigate their evolution under different parameter settings and even in more complex nonlinear wave structures (Nik Ismail & Alias, 2019; Alias et al., 2019; Nik Ismail et al., 2020; Alrzqi et al., 2024; Shamshu, et al., 2025). However, in this approach, nonlinear products are evaluated in physical space and subsequently transformed into Fourier space. This procedure may generate unresolved high-frequency modes, leading to aliasing errors that contaminate the numerical solution. The standard 2/3 dealiasing rule is particularly relevant for nonlinear pseudospectral calculations because nonlinear mode interactions can transfer energy into high-frequency components that are not adequately represented by the computational grid (Hou & Li, 2007; Bardos & Tadmor, 2015). The importance of adequate spatial resolution in obtaining reliable numerical solutions has been highlighted previously to assess the accuracy and error behaviour of spectral and pseudospectral methods for KdV-type equations (Bardos & Tadmor, 2015; Sang & Wu, 2024). Besides, spatial resolution is also important in obtaining reliable pseudospectral solutions as an inadequate number of spatial points may fail to capture localized wave profiles, steep gradients, or small-scale oscillations.

Although existing studies have developed numerous numerical approaches for KdV-type equations, there is still value in systematically examining how changes in the relative strength of nonlinear and dispersive terms affect the computed wave structures within a consistently dealiased Fourier pseudospectral framework, particularly with respect to spatial resolution and periodic-domain effects. In this study, a fully non-dimensionalised KdV equation is solved using a Fourier pseudospectral solver developed in C programming with FFT-based spatial differentiation and the 2/3 dealiasing rule. A grid-resolution study is first conducted using different numbers of spatial points to assess the adequacy of the spectral resolution. The spatial resolution, N=4096 is then adopted throughout the subsequent simulations and three representative parameter regimes are then studied. First, a balanced case is considered as a validation problem. Second, nonlinear-dominated cases are investigated by increasing μ, while maintaining λ, with the wave evolution is visualized using three-dimensional space–time plots to demonstrate wave steepening and soliton fission. Third, dispersion-dominated cases are examined by increasing λ relative to μ, where the wave evolution illustrates amplitude reduction, dispersive spreading, and oscillatory structures. Through the combination of grid-resolution assessment, dealiasing, and three-dimensional visualization, this study systematically evaluates the capability of the Fourier pseudospectral method to resolve different wave behaviours arising from changes in the nonlinear–dispersive balance and systematically map the exact grid thresholds requires to eliminate boundary reflections and numerical noise.

Methodology

The methodology is structured into four components. Initially, the Fourier pseudospectral discretization and time integration scheme is formulated to evaluate the spatial and temporal derivatives followed by the explanation of the dealiasing rule used to supress high-frequency numerical errors. Third, the computational parameters used for simulation is defined. Lastly, the numerical validation is performed to ensure the accuracy.

Fourier Pseudospectral Discretization and Time Integration

The Fourier pseudospectral method employed in this study uses the Discrete Fourier Transform (DFT) to represent the solution in a periodic computational domain. Spatial derivatives are evaluated in Fourier space, while the Fast Fourier Transform (FFT) is used to efficiently

Copyright © Academic Inspired Network
- All rights reserved

This work is licensed under
CC BY 4.0

Volume: 11 Issues: 87 Special Issue [October, 2026] pp 951-965
Journal of Islamic, Social, Economics and Development (JISED)
eISSN: 0128-1755
Journal website: academicinspired.com/jised
DOI: 10.55573/JISED.118765

perform transformations between the physical and spectral representations (Cooley & Tukey, 1965; Rashid, 2006; Jiang et al., 2023). In the PS approach, the spatial derivatives are evaluated in Fourier space, whereas the nonlinear terms are computed in physical space. The temporal derivative is subsequently discretised using a finite-difference scheme.

To formulate the numerical scheme, the KdV equation (1) is first considered over an infinite spatial domain. The infinite interval, $-L < x < L$ is truncated to a finite computational domain, which is subsequently represented as a periodic interval. Let the computational domain be defined by $[0, 2\pi]$. By introducing $\xi = sx + \pi$, the KdV equation, $A(x,t)$ is now transformed into its periodic form, $A(\xi,t)$ as:

$$A_t + \mu s A A_\xi + \lambda s^3 A_{\xi\xi\xi} = 0 \quad (3)$$

For convenience, the nonlinear terms are denoted by $W(\xi,t) = \frac{1}{2} sA^2$. Thus, equation (3) can be expressed in the following simplified form:

$$A_t + \mu W_\xi + \lambda s^3 A_{\xi\xi\xi} = 0 \quad (4)$$

The periodic spatial interval $[0, 2\pi]$ is then discretised using N uniformly distributed grid points. Let $\xi_0 = 0, \xi_1, \xi_2, ..., \xi_N = 2\pi,$ such that In this implementation, N is selected as a power of two to facilitate efficient computation using the FFT. The spatial grid points are defined by $m = \frac{N}{2}$. The DFT of the numerical solution $A(\xi_j, t)$ is then introduced. For $j = 0, 1, 2, ..., N-1,$ the discrete Fourier coefficients are defined as $A(p,t)$ denoted by:

$$A(p,t) = F(A) = \frac{1}{\sqrt{N}} \sum_{j=0}^{N-1} A(\xi_j, t) e^{-\left(\frac{2\pi jp}{N}\right) i}$$

where $p = -m, -m+1, -m+2, ..., m-1$ and $i = \sqrt{-1},$ the usual imaginary number and p is an integer. The corresponding inverse Fourier transform of $A(p,t)$ denoted by $A(\xi,t)$ is given by:

$$A(\xi_j, t) = F^{-1}(A) = \frac{1}{\sqrt{N}} \sum_{p=-m}^{m-1} A(p,t) e^{\left(\frac{2\pi jp}{N}\right) i}$$

where the DFT and inverse DFT are denoted by $F(A)$ and $F^{-1}(A)$ respectively. The spatial derivatives of $A(x,t)$ can then be evaluated efficiently in Fourier space. Differentiation with respect to x is performed by multiplying the corresponding Fourier coefficients by the wavenumber, such that

$$\frac{\partial^n A}{\partial x^n} = F^{-1}\left\{(ip)^n F\{A\}\right\}, n = 1, 2, \ldots \quad (5)$$

Copyright © Academic Inspired Network
- All rights reserved

This work is licensed under
CC BY 4.0

Volume: 11 Issues: 87 Special Issue [October, 2026] pp 951-965
Journal of Islamic, Social, Economics and Development (JISED)
eISSN: 0128-1755
Journal website: academicinspired.com/jised
DOI: 10.55573/JISED.118765

Applying the DFT to equation (4) with respect to the spatial variable ξ yields

$$A_t + i\mu pW - i\lambda(sp)^3 A = 0 \quad (6)$$

where the hat notation denotes the Fourier-transformed quantity. The temporal discretisation is subsequently introduced using the following finite-difference approximation:

$$A_t \approx \frac{A(p,t+\Delta t) - A(p,t-\Delta t)}{2\Delta t} = \frac{A^{k+1} - A^{k-1}}{2\Delta t}$$

$$A \approx \frac{A(p,t+\Delta t) + A(p,t-\Delta t)}{2} = \frac{A^{k+1} + A^{k-1}}{2} \quad (7)$$

Subtitute equation (7) into equation (6), gives

$$\left[\frac{A^{k+1} - A^{k-1}}{2\Delta t}\right] + i\mu pW - i\lambda(sp)^3 \left[\frac{A^{k+1} - A^{k-1}}{2}\right] = 0 \quad (8)$$

and, hence, the forward time-stepping scheme for the KdV equation is obtained as

$$A^{k+1} = \frac{A^{k-1}\left[1 + \lambda i(sp)^3(\Delta t)\right] - 2\mu ipW(\Delta t)}{1 - \lambda i(sp)^3(\Delta t)} \quad (9)$$

Equation (9) represents a three-level finite-difference scheme, in which the solution at the next time level depends on the solutions at two previous time levels. Therefore, both the initial time level and the second time level are required to initiate the computation.

The initial condition provides the solution at the first-time level. However, the third level, A^{k+1} cannot be directly obtained from the three-level scheme because it requires both the initial condition, A^{k-1} and the second time level, A^k. To overcome this starting-step problem and improve numerical stability, the first time step is divided into ten smaller sub-steps. Thus, the initial time step is divided by ten to obtain the smaller time increment, Δt. The corresponding second time level is then calculated using

$$A^k = \frac{A^{k-1}\left[1 + \lambda i(sp)^3\left(\frac{\Delta t}{10}\right)\right] - 2\mu ipW\left(\frac{\Delta t}{10}\right)}{1 - \lambda i(sp)^3\left(\frac{\Delta t}{10}\right)} \quad (10)$$

Since the interval between A^{k-1} and A^k is divided into ten sub-intervals, the corresponding numerical scheme is evaluated ten times to obtain the solution at the required second time level, The resulting solution is subsequently used to initialise the three-level forward scheme for the remaining time integration.

Copyright © Academic Inspired Network
- All rights reserved

This work is licensed under
CC BY 4.0

Volume: 11 Issues: 87 Special Issue [October, 2026] pp 951-965
Journal of Islamic, Social, Economics and Development (JISED)
eISSN: 0128-1755
Journal website: academicinspired.com/jised
DOI: 10.55573/JISED.118765

Dealiasing

A dealiasing technique is employed to reduce aliasing errors arising from the nonlinear terms. In the pseudospectral method, nonlinear products are evaluated in physical space and subsequently transformed into Fourier space that generates unresolved high-frequency modes that may be aliased into lower wavenumbers and contaminates the numerical solution. Specifically, the discrete physical wavenumbers are mapped using:

$$p = j - \frac{N}{2} \quad (11)$$

The standard 2/3 dealiasing rule is then applied to minimize this effect by removing the upper one-third of the Fourier modes before time integration. The zero-mask filter condition for removing these high-frequency components is mathematically defined as:

$$A(p,t) = 0, \text{ for } |p| > \frac{N}{3} \quad (12)$$

This procedure suppresses spurious spectral components and enhances the accuracy and reliability of the numerical solution for nonlinear wave propagation.

Computational Parameters

The numerical simulations were carried out using the parameters listed in Table 1. These parameters define the computational domain, spatial and temporal discretization, and initial wave amplitude uses throughout the simulation. The computational domain and discretization parameters are selected to provide sufficient numerical resolution for capturing the propagation of solitary waves and to ensure stable and accurate numerical solutions using Fourier pseudospectral method.

Table 1: Computational and numerical parameters utilized in the simulation.

Parameter	Description	Value
L	Computational Domain	500 & 1500
N	Number of Spatial Grid Points	128, 512, 2048 & 4096
Δx	Spatial Step Size	$2L/N$
Δt	Time Step Size	0.001
t_{max}	Final Simulation Time	20
a_0	Initial Wave Amplitude	1
μ_0	Initial Nonlinear Effect	6
λ_0	Initial Dispersion Effect	1

Spatial Resolution and Numerical Validation

The scheme was successfully implemented in c programming. For the benchmark case, the coefficients were set to μ=6 and λ=1, corresponding to the classical KdV configuration and allowing comparison with the analytical solitary-wave solution. Since the accuracy of pseudospectral methods depends strongly on spatial resolution, a grid-refinement study was first conducted using N=128, 512, and 2048 spatial points as an insufficient number of Fourier modes may fail to adequately resolve the nonlinear and dispersive structures of the solution. Therefore, an investigation of the influence of the number of spatial grid points N is necessary

Copyright © Academic Inspired Network
- All rights reserved

This work is licensed under
CC BY 4.0

Volume: 11 Issues: 87 Special Issue [October, 2026] pp 951-965
Journal of Islamic, Social, Economics and Development (JISED)
eISSN: 0128-1755
Journal website: academicinspired.com/jised
DOI: 10.55573/JISED.118765

to establish the reliability and convergence of the numerical solution. Figure 1 shows the the numerical solution of KdV equation (1), with parameters according to Table 1 for different data size, N where the initial condition from (2) is given by:

$$A(x,0) = \sec h^2(kx), \qquad k = (1/2)^{1/2} \quad (13)$$

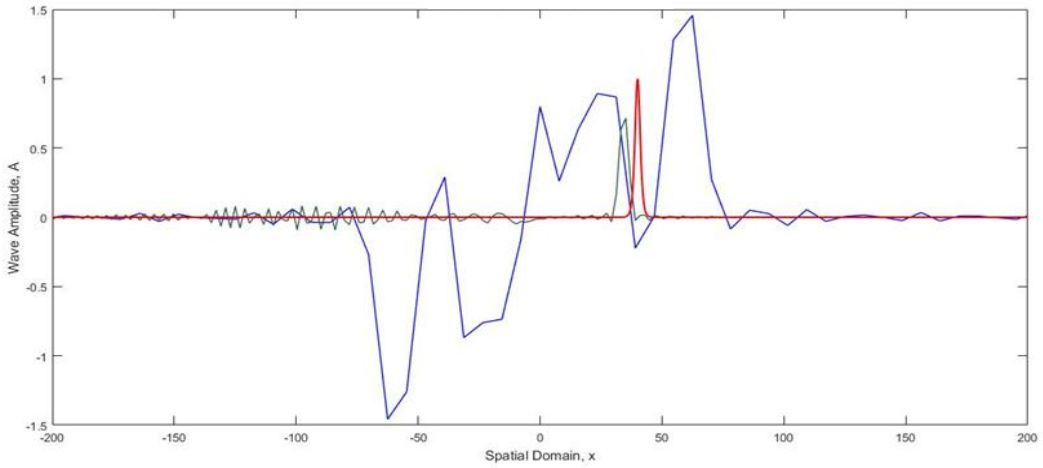

Figure 1: Comparison of the numerical solutions of equation (1) for different spatial resolutions, *N*. The blue line is for *N*=128, green line is *N*=512 and the red line is for *N*=2048.

Figure 1 compares the numerical solutions at t=20 for the three spatial resolutions. At N=128, noticeable oscillations and an insufficiently resolved wave profile are observed. These oscillations are reduced significantly by increasing the resolution to N=512 and a clearer wave structure is observed. At N=2048, the solution becomes smooth and well resolved, with no visible numerical oscillations. These results demonstrate the importance of sufficient spatial resolution in resolving the wave dynamics.

Comparative numerical results for the amplitude, a, and the phase speed, c, of the wave for N=2048 and 4096 are given in Table 2. The empirical results clearly demonstrate that the N=4096 mesh configuration provides superior structural accuracy over N=2048. For N=2048 grid, the amplitude experiences a larger deviation to a = 0.971345 at t=5. The N=4096 solution, in contrast, successfully eliminates this numerical damping, keeping the amplitude threshold of a = 0.999999, bringing the spatial discretization error to a near 0.00%. The phase-speed, c results for the same resolution also reveal smaller deviations for the finer resolution where x_{peak} denotes the coordinates where the wave amplitude reaches its maximum.

Copyright © Academic Inspired Network
- All rights reserved

This work is licensed under
CC BY 4.0

Volume: 11 Issues: 87 Special Issue [October, 2026] pp 951-965
Journal of Islamic, Social, Economics and Development (JISED)
eISSN: 0128-1755
Journal website: academicinspired.com/jised
DOI: 10.55573/JISED.118765

Table 2: The numerical solution of amplitude, *a* and phase speed, *c* of solitary waves, calculated for *N*=2048 and 4096

t	*N*=2048		*N*=4096	
	a	$c = x_{peak}/t$	*a*	$c = x_{peak}/t$
1	0.997854	1.953125	0.998611	1.953125
2	0.994335	1.953125	0.995026	1.953125
3	0.988717	1.953125	0.995287	2.034505
4	0.981033	1.953125	0.998736	2.014160
5	0.971345	1.953125	0.999999	2.001953
6	0.979501	2.034505	0.999066	1.993815
7	0.987537	2.022879	0.995944	1.988002
8	0.993516	2.014160	0.994300	2.014160
9	0.997385	2.007378	0.998199	2.007378
10	0.999124	2.001953	0.999917	2.001953

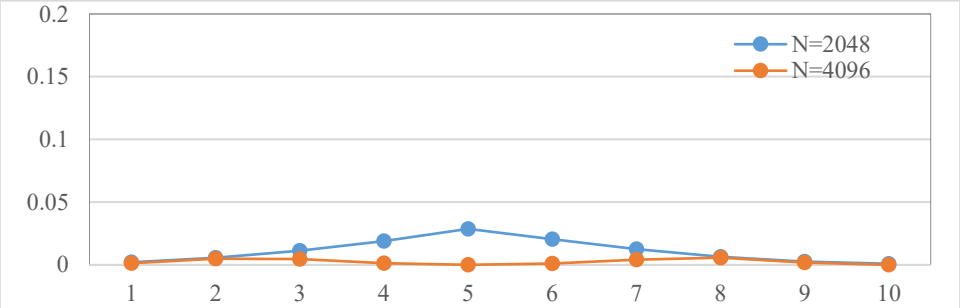

Figure 2: Absolute numerical error convergence in amplitude, *a*, for indicates spatial sizes over time.

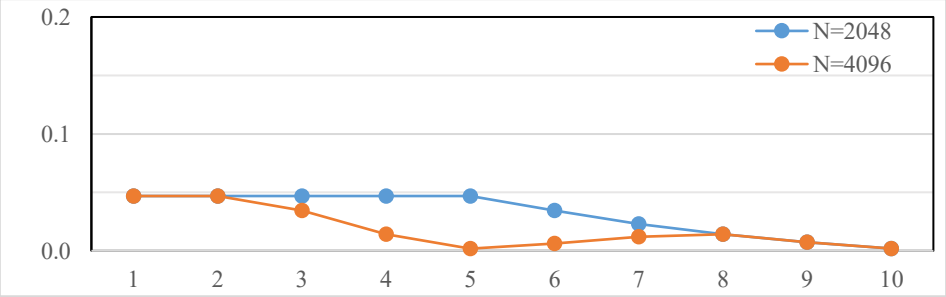

Figure 3: Absolute numerical error in phase speed, *c*, for indicates spatial sizes over time.

The absolute error in amplitude and phase speed are illustrated in Figures 2 and 3, respectively using:

$$Error = \left| E_{exact} - E_{numerical} \right| \quad (14)$$

The *N*=2048 grid yields relatively larger errors, particularly around *t*=5, while the *N*=4096 grid yields more accurate results that are consistent with the expected solitary-wave behaviour These results confirm that increasing the spatial resolution improves the accuracy of the numerical solution. Based on this resolution assessment, the subsequent simulations, *N*=4096 is used for the following nonlinear and dispersive parameter combination.

Copyright © Academic Inspired Network
- All rights reserved

This work is licensed under CC BY 4.0

Volume: 11 Issues: 87 Special Issue [October, 2026] pp 951-965
Journal of Islamic, Social, Economics and Development (JISED)
eISSN: 0128-1755
Journal website: academicinspired.com/jised
DOI: 10.55573/JISED.118765

Results and Discussion

This section presents the numerical simulation result for KdV equation across three distinct physical regimes. For validation, a balanced case is first examined to show a stable propagation of the solitary wave. Secondly, nonlinear dominated regimes are discussed by increasing the nonlinear parameter, highlighting phenomena like wave steepening and soliton fission. Finally, dispersion dominated regimes are examined where the evolution of waves is characterized by amplitude decay, dispersive spreading, and the generation of oscillatory structures.

Case 1: Stable Solitary-Wave Propagation

The balanced case is considered as a validation test of the numerical implementation and parameter selection. For the parameters μ=6 and λ=1, the nonlinear and dispersive effects are balanced and a stable solitary wave of amplitude, a=1 and propagation speed, c=2 is obtained using Equation (2). The amplitude of the wave remains constant throughout the propagation, and the wave remains localised in its shape as shown in Figure 4. The similarity of the numerical amplitude and phase speed to the expected values validates the use of Fourier pseudospectral scheme and the chosen set of numerical parameters to capture the typical features of the KdV solitary wave.

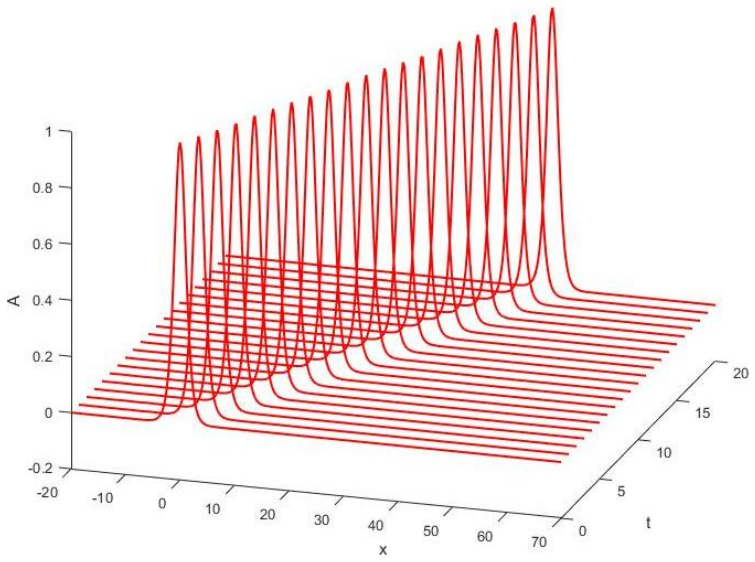

Figure 4: The propagation of the solitary wave up to the end time t=20 in 3D space–time profile.

Case 2: Soliton Fission in the Nonlinearity, ($\mu > \lambda$)

The second case investigates the effect of increasing the nonlinear parameter, μ while maintaining λ =1, with μ =12 and 24. Here, the initial solitary wave is significantly distorted, as shown in Figures 5 and 6, in contrast to the balanced regime.

Copyright © Academic Inspired Network
- All rights reserved

This work is licensed under
CC BY 4.0

Volume: 11 Issues: 87 Special Issue [October, 2026] pp 951-965
Journal of Islamic, Social, Economics and Development (JISED)
eISSN: 0128-1755
Journal website: academicinspired.com/jised
DOI: 10.55573/JISED.118765

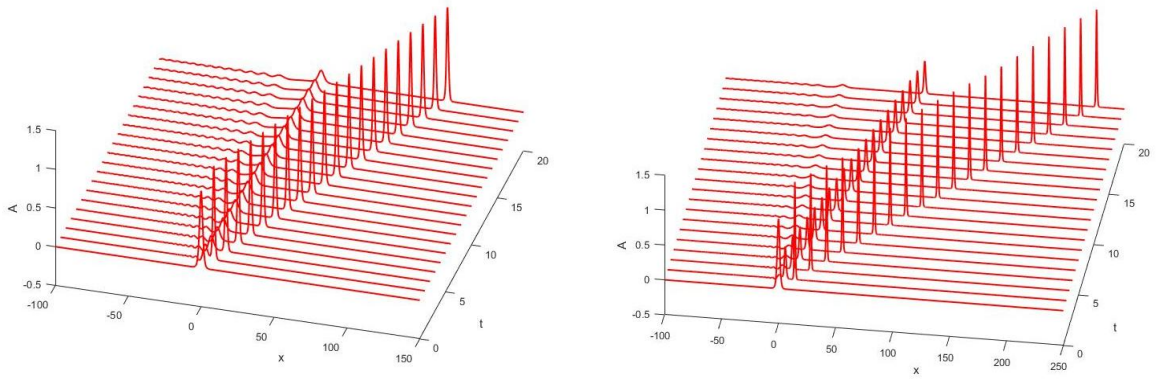

Figure 5: Spatial-temporal wave propagation in the nonlinear-dominated regimes for μ =12 (Left) and μ=24 (Right), plotted at every t=1.

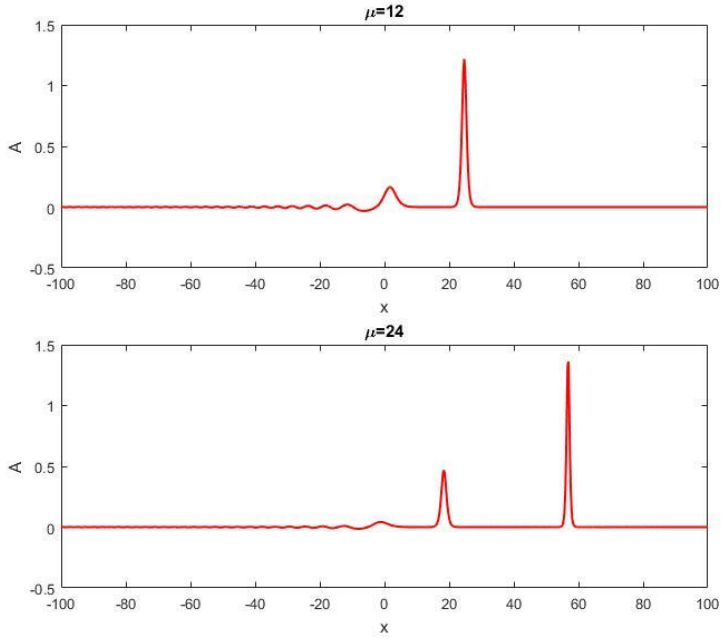

Figure 6: 2D cross-sectional profiles of solitary wave fissioning at t=5 for indicated nonlinear coefficient, μ.

Figures 5 and 6 demonstrate that for larger values of μ, the nonlinear steepening is enhanced and then soliton fission is accentuated. The initial wave evolves into multiple localized wave components with different amplitudes and propagation speeds. As the nonlinear coefficient, μ, increases from 12 to 24, the fission becomes more distinct, which shows the significant effect of the nonlinear coefficient on the evolution of the wave. The peak amplitude increases from about 1.14 to 1.36 because of the fission process, while the resulting wave components exhibit distinct propagation speeds, c. Overall, the higher-amplitude waves propagate faster than the lower-amplitude waves, which is consistent with the nonlinear amplitude–speed relationship of KdV solitary waves.

The results also show the capability of the Fourier pseudospectral method to resolve the complex structures that arise in the evolution of nonlinear waves. The fission process gives rise to several localised structures and steeper spatial variations as compared to the smooth profile of the balanced regime. These features are resolved sufficiently using N=4096, where the evolution and separation of the wave components can be clearly captured. Overall, these results

Copyright © Academic Inspired Network - All rights reserved

This work is licensed under CC BY 4.0

Volume: 11 Issues: 87 Special Issue [October, 2026] pp 951-965
Journal of Islamic, Social, Economics and Development (JISED)
eISSN: 0128-1755
Journal website: academicinspired.com/jised
DOI: 10.55573/JISED.118765

show that higher values of the nonlinear coefficient alter the dynamics of the wave from a stable solitary-wave propagation towards stronger steepening and soliton fission.

Case 3: Dispersive Radiation in the Dispersion-Dominated Regime ($\lambda > \mu$)

Figure 7 further illustrates the effect of increasing the dispersion coefficient while maintaining μ. The figure shows a severe periodic wrap-around reflection caused by an under-optimized domain length of L=500. As oscillatory features developed, the trailing radiation propagates toward the negative boundary and re-enters the computational domain via the periodic boundary condition. This recurrence introduces a non-physical numerical interaction that contaminate the wave profile.

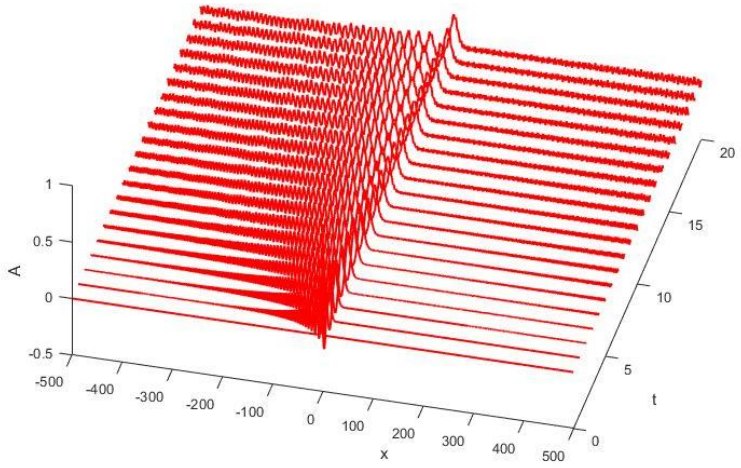

Figure 7: Unoptimized spatial domain layout at L=500. The profile displays severe spatial-temporal wave distortion caused by periodic boundary wrap-around reflections.

To minimize this boundary effect while maintaining a practical computational cost, the spatial domain is extended to L=1500, as indicated in Figure 8. The larger domain will allow sufficient space for the dispersive radiation to propagate until it reaches the periodic boundaries. The solution obtained shows a more distinct development of the dispersive wave structure, with the oscillatory radiation tail developing behind without significant interference from boundary wrap-around. The domain refinement shows the necessity of choosing an appropriate computational domain when simulating strongly dispersive wave propagation using a Fourier pseudospectral method.

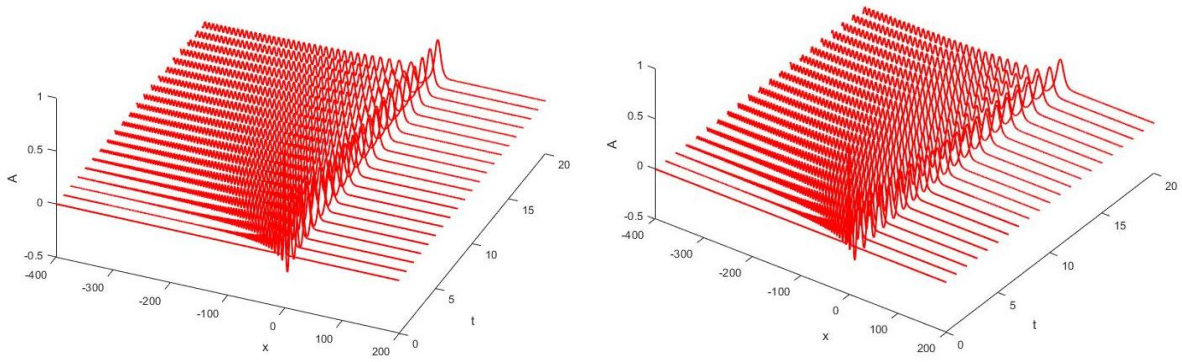

Figure 8: Optimized spatial domain layout extended to L=1500 for λ = 8 (left) and 12 (Right). The dispersive shock wave profile and the tail of trailing radiation are physically resolved in the right domain.

Copyright © Academic Inspired Network - All rights reserved

This work is licensed under CC BY 4.0

Volume: 11 Issues: 87 Special Issue [October, 2026] pp 951-965
Journal of Islamic, Social, Economics and Development (JISED)
eISSN: 0128-1755
Journal website: academicinspired.com/jised
DOI: 10.55573/JISED.118765

Figure 8 further illustrates the effect of increasing the dispersion coefficient from $\lambda = 8$ to $\lambda = 12$ while maintaining μ=6. As dispersion becomes increasingly dominant, the initial localized wave undergoes greater spreading and develops pronounced wave trains around the main pulse. The maximum amplitude decreases, while the trailing dispersive wave train becomes more extended and structurally complex. The two-dimensional cross-sectional profiles corresponding to Figure 8 at time t=5 is shown in Figure 9.

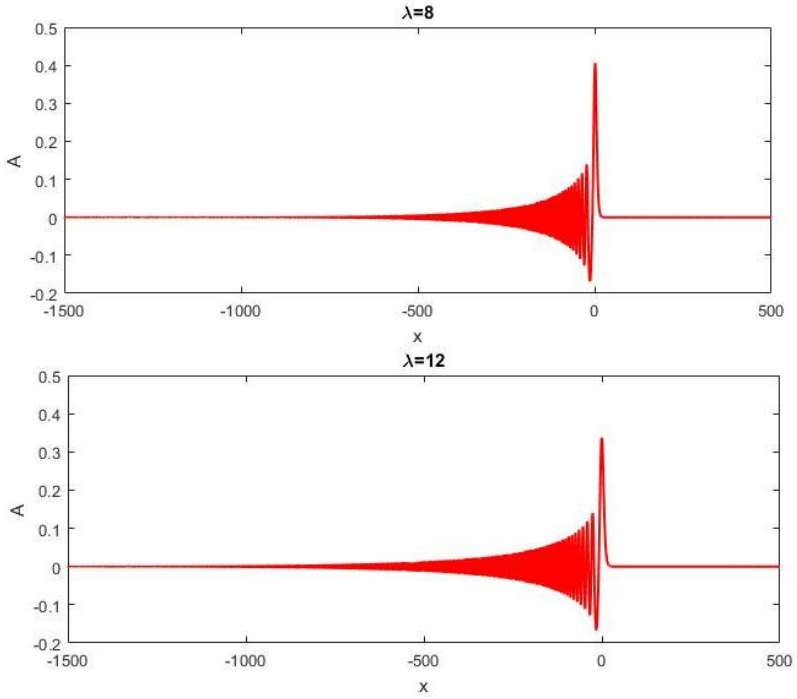

Figure 9: Cross-sectional solitary wave profiles at t=5 for indicated dispersion coefficient, λ.

Figure 9 shows that increasing λ from 8 to 12 reduces the peak amplitude from approximately 0.41 to 0.34. This reduction is associated with stronger dispersive spreading, making the wave less spatially concentrated. A distinct change in the trailing oscillatory structure is also observed. The oscillations in the radiation tail are more closely spaced for λ =12 than λ =8, indicating that the spatial structures are more refined for larger dispersion. The Fourier pseudospectral method can resolve these oscillatory structures with good resolution of the main wave and its dispersive tails.

Overall, the three numerical regimes demonstrate the ability of the Fourier pseudospectral method to resolve distinctly different nonlinear dispersive wave behaviours. The balanced regime gives rise to stable propagation of solitary waves, the nonlinear-dominated regime results in wave steepening and wave fission, and the dispersion-dominated regime gives rise to spreading of the amplitude and growing oscillatory radiation. These results, together with the grid-resolution assessment and application of the 2/3 dealiasing rule, show that the proposed pseudospectral framework is appropriate for the simulation of nonlinear wave propagation in a variety of nonlinear and dispersive parameter regimes.

Copyright © Academic Inspired Network - All rights reserved

This work is licensed under CC BY 4.0

Volume: 11 Issues: 87 Special Issue [October, 2026] pp 951-965
Journal of Islamic, Social, Economics and Development (JISED)
eISSN: 0128-1755
Journal website: academicinspired.com/jised
DOI: 10.55573/JISED.118765

Conclusion

The grid-resolution study showed that a higher number of grid spatial points leads to higher resolution and accuracy of the wave profile computed. In view of this, N=4096 was adopted in the following simulations for adequate resolution of the various wave structures resulting from the different values of the nonlinear and dispersive coefficients. The numerical results showed that there are three different types of wave behaviours. The numerical solution was able to reproduce the stable propagation of the solitary waves, and the amplitude was approximately 1, the propagation speed c=2 for the case of a balanced KdV equation with normalized KdV equation parameters, μ=6 and λ=1. The relative amplitude error at t=5 is 0.00%, which gets quantitative evidence of the accuracy of the numerical implementation. As the nonlinear coefficient is raised, the progressive wave steepening, and soliton fission occur, leading to several localized waves with different amplitude and propagation speeds. Conversely, the amplitude decreased, the spatial spread increased and finer and more intricate oscillatory structures formed in the dispersive tail as the dispersion coefficient was increased.

In general, the results show that the Fourier pseudospectral method with the proper spatial resolution and 2/3 dealiasing can be used to accurately describe a wide variety of nonlinear dispersive wave phenomena, such as stable propagation of solitary waves, soliton fission, and dispersive spreading. The framework therefore provides a reliable numerical approach for investigating parameter-dependent wave dynamics in KdV-type equations. Future studies can extend the developed computational framework to model more complex non-linear wave systems to provide valuable insights into the multi-physical interactions.

Acknowledgements

The authors would like to acknowledge Universiti Teknologi MARA (UiTM) and Universiti Malaysia Terengganu (UMT) for providing the institutional support and computational facilities that made this collaborative research possible.

Copyright © Academic Inspired Network
- All rights reserved

This work is licensed under
CC BY 4.0

Volume: 11 Issues: 87 Special Issue [October, 2026] pp 951-965
Journal of Islamic, Social, Economics and Development (JISED)
eISSN: 0128-1755
Journal website: academicinspired.com/jised
DOI: 10.55573/JISED.118765

References

Ablowitz M. J., Cole J. T., El, G. A., Hoefer, M. A, & Luo X-D. (2023). Soliton–mean Field Interaction in Korteweg–de Vries Dispersive Hydrodynamics. *Studies in Applied Mathematics*. 151(3), 795–856. https://doi.org/10.1111/sapm.12615

Alias, A., Ismail, N. N. A. N. & Harun, F. N. (2019). Pseudospecteral Method with Linear Damping Effect and De-aliasing Technique in Solving Nonlinear PDEs. *Journal of Physics Conference Series*, 1366(1), 012009. https://doi.org/10.1088/1742-6596/1366/1/012009

Alomair, A., Al Naim, A. S., & Bekir, A. (2025). Exploration of Soliton Solutions to the Special Korteweg–de Vries Equation with Stability Analysis and Modulation Instability. *Mathematic*s, 13(1), 54. https://doi.org/10.3390/math13010054

Alrzqi, S. F., Alrawajeh, F. A., & Hassan, H. N. (2024). An Efficient Numerical Technique for Investigating the Generalized Rosenau-KDV-RLW Equation by Using the Fourier Spectral Method. *AIMS Mathematics*, 9(4), 8661–8688. https://doi.org/10.3934/math.2024420

Bardos, C. & Tadmor, E. (2015). Stability and Spectral Convergence of Fourier Method for Nonlinear Problems: On the Shortcomings of the 2/3 De-Aliasing Method. *Numerische Mathematik*, 129, 749–782. https://doi.org/10.1007/s00211-014-0652-y

Biswas, A., Ketcheson, D. I., Ranocha, H. & Schütz, J. (2025). Traveling-Wave Solutions and Structure-Preserving Numerical Methods for a Hyperbolic Approximation of the Korteweg-de Vries Equation. *Journal of Scientific Computing*, 103(90). https://doi.org/10.1007/s10915-025-02898-x

Cheng, S. & Liu, H. (2023). Weakly Nonlinear Waves Over the Bottom Disturbed Topography: Korteweg–De Vries Equation with Variable Coefficients. *European Journal of Mechanics – B/Fluids*, 98, 238–246. https://doi.org/10.1016/j.euromechflu.2022.12.010

Cooley, J. W., & Tukey, J. W. (1965). An Algorithm for the Machine Calculation of Complex Fourier Series. *Mathematics of Computation,* 19, 297–301https://doi.org/10.2307/2003354

Congy, T., El, G. A., Roberti, G. & Tovbis, A. (2023). Dispersive Hydrodynamics of Soliton Condensates for the Korteweg–De Vries Equation. *Journal of Nonlinear Science*. 33(104). https://doi.org/10.1007/s00332-023-09940-y

Dwivedi, M. & Sarkar, T. (2025). Convergence of a Conservative Crank–Nicolson Finite Difference Scheme for the KdV Equation. *Mathematical Methods in the Applied Sciences,* 48(17), 15602–15619. https://doi.org/10.1002/mma.70035

Hou, T. Y. & Li, R. (2007). Computing Nearly Singular Solutions Using Pseudo-Spectral Methods. *Journal of Computational Physics,* 226(1), 379-397. https://doi.org/10.1016/j.jcp.2007.04.014

Irawan, D. E., Herho, S. H. S., Pamumpuni, A., Kartiko, R. D., Khadami, F., Anwar, I. P., Sujatmiko, K. A., Handayani, A. P., Fajary, F. R., & Suwarman R. (2026). An Open-source Pseudo-Spectral Solver for Idealized Korteweg–de Vries Soliton Simulations. *Water*. 18(7), 779. https://doi.org/10.3390/w18070779

Jiang, C., Cui, J., Cai, W. & Wang, Y. (2023). A Novel Linearized and Momentum-Preserving Fourier Pseudo-Spectral Scheme for the Rosenau-Korteweg de Vries Equation. *Numerical Methods for Partial Differential Equation*, 39(2), 1558–1582. https://doi.org/10.1002/num.22945

Klein, C., Prada-Malagon, J., & Stoilov, N. (2023). On Numerical Approaches to Nonlinear Schrödinger and Korteweg–de Vries Equations for Piecewise Smooth and Slowly Decaying Initial Data. *Physica D: Nonlinear Phenomena*, 454, 133885. https://doi.org/10.1016/j.physd.2023.133885

Korteweg, D. J. & de-Vries, G. (1895). On the Change of Form of Long Waves Advancing in a Rectangular Canal, and on a New Type of Long Stationary Waves. *Philosophical Magazine,* 39(240), 422-443 (1895).

Copyright © Academic Inspired Network - All rights reserved

This work is licensed under CC BY 4.0

Volume: 11 Issues: 87 Special Issue [October, 2026] pp 951-965
Journal of Islamic, Social, Economics and Development (JISED)
eISSN: 0128-1755
Journal website: academicinspired.com/jised
DOI: 10.55573/JISED.118765

Singh, P. & Senthilnathan, K. (2024). Evolution of A Solitary Wave: Optical Soliton, Soliton Molecule and Soliton Crystal. *Discover Applied Science*, 464(6). https://doi.org/10.1007/s42452-024-06152-1

Nik Ismail, N. N. A. & Alias, A. (2019). Solving Variable Coefficient Korteweg-de Vries Equation Using Pseudospectral Method. *ASM Science Journal*, 12(5), 26-33.

Nik Ismail, N. N. A, Alias, A. & Harun, F. N. (2020). The Propagation of Nonlinear Internal Waves Under the Influence of Variable Topography and Earth's Rotation in a Two-Layer Fluid. *Fluids*, 5(3), 140. https://doi.org/10.3390/fluids5030140

Rashid, A. (2006). Convergences Analysis of Three-Level Fourier Pseudospectral Method for Korteweg-de Vries Burgers Equation. *An International Journal Computers and Mathematics with Applications*, 52(5), 769-778.https://doi.org/10.1016/j.camwa.2006.10.014

Sang, L. & Wu, H. (2024). Error Estimates of a Space–time Legendre Spectral Method for Solving the Korteweg–de Vries Equation. *Communications in Nonlinear Science and Numerical Simulation*, 133, 107991. https://doi.org/10.1016/j.cnsns.2024.107991

Salian, L. V., Samala, R. & Ghosh, D. (2026). Central Compact Finite-difference Scheme with High Spectral Resolution for KdV Equation. *Numerical Methods for Partial Differential Equations*, 42(1), e70060. https://doi.org/10.1002/num.70060

Shamshu, N. M. L. K., Alias, A., & Loy, K. C. (2025). Numerical Solution of Extended Korteweg-De Vries Equation with Cubic Nonlinear Term and Fifth-Order Dispersion Term. *Malaysian Journal of Mathematical Sciences*. 19(1), 163–176. https://doi.org/10.47836/mjms.19.1.09

Wang, Z., Wei, Q. & Zhang, Q. (2025). Some Discontinuous Galerkin Schemes for Korteweg-De Vries Equations: Error Estimates and Application. *Numerical Methods for Partial Differential Equation*, 41(4), e70011. https://doi.org/10.1002/num.70011

Copyright © Academic Inspired Network - All rights reserved

This work is licensed under CC BY 4.0